The GLP-1R agonist liraglutide limits hepatic lipotoxicity and inflammatory response in mice fed a methionine-choline deficient diet

Somm, Emmanuel; Montandon, Sophie Anne; Loizides-Mangold, Ursula Elfriede; Gaia, Nadia; Lazarevic, Vladimir; De Vito, Claudio; Perroud, Elodie Nathalie; Piallat, Marie-Luce; Dibner, Charna; Schrenzel, Jacques; Jornayvaz, François

How to cite

SOMM, Emmanuel et al. The GLP-1R agonist liraglutide limits hepatic lipotoxicity and inflammatory response in mice fed a methionine-choline deficient diet. In: Translational Research, 2020. doi: 10.1016/j.trsl.2020.07.008

This publication URL: https://archive-ouverte.unige.ch/unige:139520

Publication DOI: 10.1016/j.trsl.2020.07.008

The GLP-1R agonist liraglutide limits hepatic lipotoxicity and inflammatory response in mice fed a methionine-choline deficient diet

EMMANUEL SOMM[1], SOPHIE A. MONTANDON[1], URSULA LOIZIDES-MANGOLD, NADIA GAÏA, VLADIMIR LAZAREVIC, CLAUDIO DE VITO, ELODIE PERROUD, MARIE-LUCE BOCHATON-PIALLAT, CHARNA DIBNER, JACQUES SCHRENZEL, and FRANÇOIS R. JORNAYVAZ

GENEVA, SWITZERLAND

Nonalcoholic fatty liver disease (NAFLD) is the most common hepatic disorder related to type 2 diabetes (T2D). The disease can evolve toward nonalcoholic steatohepatitis (NASH), a state of hepatic inflammation and fibrosis. There is presently no drug that effectively improves and/or prevents NAFLD/NASH/fibrosis. GLP-1 receptor agonists (GLP-1Ra) are effective in treating T2D. As with the endogenous gut incretins, GLP-1Ra potentiate glucose-induced insulin secretion. In addition, GLP-1Ra limit food intake and weight gain, additional beneficial properties in the context of obesity/insulin-resistance. Nevertheless, these pleiotropic effects of GLP-1Ra complicate the elucidation of their direct action on the liver. In the present study, we used the classical methionine-choline deficient (MCD) dietary model to investigate the potential direct hepatic actions of the GLP-1Ra liraglutide. A 4-week infusion of liraglutide (570 μg/kg/day) did not impact body weight, fat accretion or glycemic control in MCD-diet fed mice, confirming the suitability of this model for avoiding confounding factors. Liraglutide treatment did not prevent lipid deposition in the liver of MCD-fed mice but limited the accumulation of C16 and C24-ceramide/sphingomyelin species. In addition, liraglutide treatment alleviated hepatic inflammation (in particular accumulation of M1 pro-inflammatory macrophages) and initiation of fibrosis. Liraglutide also influenced the composition of gut microbiota induced by the MCD-diet. This included recovery of a normal *Bacteroides* proportion and, among the Erysipelotrichaceae family, a shift between *Allobaculum* and *Turicibacter* genera. In conclusion, liraglutide prevents accumulation of C16 and C24-ceramides/sphingomyelins species, inflammation and initiation of fibrosis

[1]These authors contributed equally to this work.

From the Service of Endocrinology, Diabetes, Nutrition and Patient Education, Department of Internal Medicine, Geneva University Hospitals/University of Geneva, Geneva, Switzerland; Diabetes Center, Faculty of Medicine, University of Geneva, Geneva, Switzerland; Department of Cell Physiology and Metabolism, University of Geneva, Geneva, Switzerland; Institute of Genetics and Genomics in Geneva (iGE3), University of Geneva, Geneva, Switzerland; Genomic Research Laboratory, Service of Infectious Diseases, Geneva University Hospitals, University of Geneva, Geneva, Switzerland; Division of Clinical Pathology, Geneva University Hospitals, Geneva, Switzerland; Department of Pathology and Immunology, Faculty of Medicine, University of Geneva, Geneva, Switzerland; Bacteriology Laboratory, Service of Laboratory Medicine, Geneva University Hospitals, Geneva, Switzerland.

Submitted for Publication February 25, 2020; received submitted July 14, 2020; accepted for publication July 16, 2020.

Reprint requests: Emmanuel Somm and François R. Jornayvaz, Service of Endocrinology, Diabetes, Nutrition and Patient Education, Department of Internal Medicine, Geneva University Hospitals/University of Geneva, Geneva, Switzerland. e-mail: emmanuel.somm@unige.ch, Francois.Jornayvaz@hcuge.ch.

1931-5244/$ - see front matter

https://doi.org/10.1016/j.trsl.2020.07.008

in MCD-diet-fed mice liver, suggesting beneficial hepatic actions independent of weight loss and global hepatic steatosis. (Translational Research 2021; 227:75–88)

Abbreviations: ALT = Alanine aminotransferase; AST = Aspartate aminotransferase; BAT = Brown adipose tissue; Cer = Ceramide; CerS = Ceramide synthase; DIO = Diet-induced obesity; FFA = Free fatty acid; GLP-1 = Glucagon like peptide-1; GLP-1Ra = GLP-1 receptor agonist; HCC = Hepatocellular carcinoma; HOMA = Homeostasis model assessment; HSC = Hepatic stellate cell; LC = Long chain; LC-MS = Liquid chromatography–mass spectrometry; Lira = Liraglutide; MCD = Methionine-choline deficient; MUFA = Monounsaturated fatty acid; NAFLD = Nonalcoholic fatty liver disease; NASH = Nonalcoholic steatohepatitis; NGS = Next generation sequencing; PUFA = Polyunsaturated fatty acid; SFA = Saturated fatty acid; SM = Sphingomyelin; T2D = Type 2 diabetes; TNF-α = Tumor necrosis factor alpha; VLC = Very long chain; WAT = White adipose tissue

Keywords: Glucagon like peptide-1 receptor agonist; Nonalcoholic fatty liver disease; Nonalcoholic steatohepatitis; Methionine-choline deficient diet; inflammation; Type 2 diabetes; Ceramide; microbiota

AT A GLANCE COMMENTARY

Emmanuel S, et al.

Background

Nonalcoholic fatty liver disease (NAFLD) and steatohepatitis (NASH) are common hepatic disorders related to type 2 diabetes (T2D). Presently, no drug effectively improves and/or prevents NAFLD/NASH/liver fibrosis. GLP-1 receptor agonists (GLP-1Ra) are effective in treating T2D but their direct action on the liver remains elusive.

Translational Significance

We presently show that infusion of the GLP-1Ra liraglutide prevents accumulation of C16 and C24-ceramides/sphingomyelins species, inflammation and initiation of fibrosis in liver from mice on a methionine-choline deficient diet, suggesting beneficial hepatic actions independent of weight loss and global hepatic steatosis. GLP-1Ra may present added-value in hepatic complications of T2D.

INTRODUCTION

Nonalcoholic fatty liver disease (NAFLD) is the most common hepatic disorder in industrialized countries.[1,2] Obesity and type 2 diabetes (T2D) are frequent causes of NAFLD.[1,2] Nevertheless, NAFLD can occur in lean patients due to various factors, including overconsumption of specific nutrients (such as fructose or cholesterol), accumulation of visceral fat, genetic predisposition, dyslipidemia, or lipodystrophy.[1,2] A significant proportion of patients with NAFLD develop a state of hepatic inflammation [nonalcoholic steatohepatitis, NASH], which can lead to fibrosis and cirrhosis, potentially resulting in hepatocellular carcinoma.[3] Whilst lifestyle changes, including a modification in eating habits, weight loss or physical activity, have beneficial effects on liver steatosis, there is currently no efficient long-term treatment available to improve and/or avoid the development and progression of NAFLD, NASH, and fibrosis.[1-3]

Studying NAFLD is challenging in humans due to the invasive nature of liver biopsies and the slow progression rate of the disease. This situation has led to the development of many animal models,[4] of which the methionine and choline deficient (MCD) diet is most frequently used.[4] The MCD diet is rich in sucrose and devoid of methionine and choline, 2 nutrients required for mitochondrial β-oxidation and very-low density lipoprotein synthesis in the liver.[5,6] As a consequence, the MCD diet induces hepatic steatosis, inflammation, and fibrosis without weight gain.[4] In addition, MCD diet-fed mice present liver-specific, but not global, insulin-resistance.[7]

Introduced about 15 years ago, GLP-1Ra are considered effective drugs for the treatment of T2D, with the advantage of limiting hypoglycemia. As does endogenous GLP-1 secreted by the enteroendocrine L-cells in the intestine, GLP-1Ra primarily potentiate glucose-induced insulin secretion.[8] In addition, GLP-1Ra protect pancreatic islets, reduce food intake, and stimulate energy expenditure,[8] all additional beneficial outcomes in the context of obesity/insulin-resistance. Interestingly, in vitro studies suggest that GLP-1Ra act directly on hepatocytes to limit endoplasmic reticulum stress,[9] activate AMP-activated protein kinase,[10-12] dampen lipogenesis[10] or interact with the insulin signaling pathways.[11-13] Nevertheless, the pleiotropic effects of GLP-1Ra on the pancreas and hypothalamus complicate the elucidation of their direct action on the liver in vivo. In fact, the antisteatotic action of GLP-1Ra has been mainly observed in situations of weight loss and/or insulin sensitization in both animal models[14-20] and humans.[21,22]

To investigate the liver-specific action of GLP-1Ra, we infused liraglutide to mice fed with the MCD diet, hypothesizing that liraglutide might improve NAFLD/NASH by reducing steatosis, inflammation and fibrosis independently of weight loss.

MATERIAL AND METHODS

Animals, diets, treatments. All experimental protocols were performed in accordance with the Swiss animal welfare laws. Fourteen-week-old C57BL/6J male mice (Charles River Laboratories) were acclimatized for 1 week in standard conditions (22°C, 12h-light/12h-dark cycle, free access to water and food). Thereafter, mice were fed with a regular chow diet (RM3, SDS; Chow group) or a MCD diet (A02082002BR, Research Diets; MCD and MCD/Lira groups) for 7 weeks. During the last 4 weeks of the experiment, mice were either infused with isotonic saline solution (Chow and MCD groups) or with liraglutide (0.1 μl/h of Victoza, Novo Nordisk [6 mg liraglutide/ml]; MCD/Lira group) via micro-osmotic pumps (Model 1004D, Alzet). Food intake and body weight were monitored weekly during the experiment. A schematic representation of the study protocol is illustrated in Fig 1. At the end of the experiment, mice were fasted 4 hours, anesthetized with isoflurane and immediately sacrificed. The osmotic pumps were retrieved and emptying was checked to confirm liraglutide release. Blood samples were collected, and organs were dissected and weighed before fixation or cryopreservation in liquid nitrogen.

Blood analyses. Blood samples were collected in EDTA-coated tubes and plasma was stored at −80°C. Plasma levels of glucose, ALT, AST, total cholesterol, triglycerides and free fatty acids were assessed using a Cobas C111 robot and appropriate reagents (Roche Diagnostics). Plasma levels of insulin were measured using an ultrasensitive mouse insulin ELISA kit (Mercodia).

Gene expression. Total RNA was isolated from 50 to 100 mg liver samples using TRI Reagent Solution (ThermoFisher). Five hundred ng of total RNA were reverse transcribed using the PrimeScript RT reagent kit (Takara) and gene expression levels were assessed by quantitative PCR using the Power SYBR Green master mix (Thermofisher) and a Light-Cycler 480 (Roche Diagnostics). Normalization was done using the 40S ribosomal protein S29 (RPS29) gene.

Histology, morphometry, pathological score. Liver and the distal part of the intestine (ileum) were either fixed overnight in 10% formalin before dehydration and embedded in paraffin or immediately embedded in OCT medium (Cell path LTD) and frozen on dry ice before storage at −80°C. Paraffin-embedded sections were stained with hematoxylin-eosin (H&E), Sirius red, Periodic Acid Schiff's solutions and Ki67 antibody using classical procedures. Frozen sections were stained with Oil red O solution using classical procedures. Pictures were acquired using a VS120 microscope (Olympus). Steatosis and fibrosis quantifications were achieved with Oil red O and Sirius red labeled slides using the area measurement tool of the ImageJ software (NIH). For fibrosis quantification, vessels, exhibiting a massive confounding collagen staining, were excluded from the analysis which represents only collagen fibers emerging in the liver parenchyma. Two independent liver lobes per animal were used for these quantifications. Ileal villi and crypt sizes were measured on H&E stained sections with the strait segment tool of ImageJ software. The pathological score, including steatosis and activity (ballooning and lobular inflammation) was evaluated by a trained pathologist (CDV) blinded to the diets as previously described.[23]

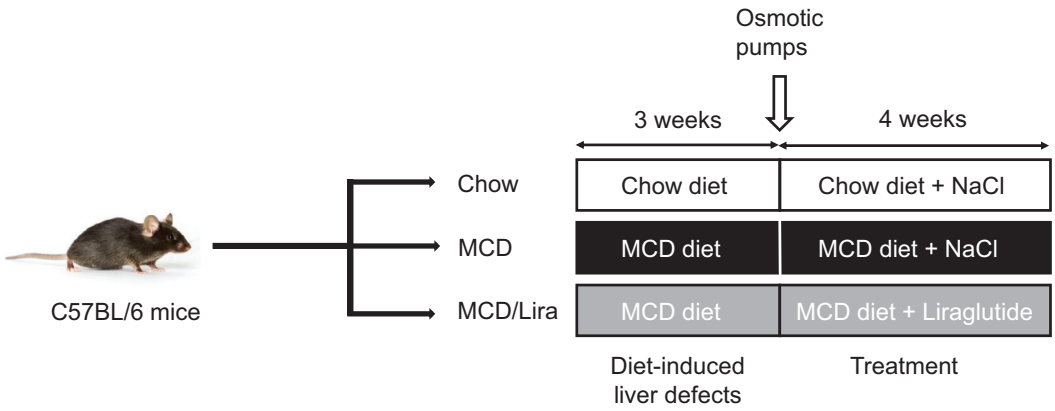

Fig 1. Schematic representation of the study protocol. Fourteen-week-old C57BL/6J male mice were fed with either a regular chow diet or a methionine-choline deficient (MCD) diet for 3 weeks to initiate liver defects mimicking human NASH. During the four last weeks of the experiment, mice were infused either with saline solution (Chow and MCD groups) or with liraglutide (6 mg/ml, 0.1 μl/h) (MCD/Lira group) via micro-osmotic pumps.

Lipidomic analysis. Lipid extraction and lipidomic analyses were performed as previously described.[24,25] Lipids were isolated from 20 mg of liver tissue. After extraction, the organic lipid containing phase was dried in a vacuum concentrator (CentriVap, Labconco). Lipids were then dissolved in chloroform/methanol and divided into 3 aliquots. One aliquot was treated by alkaline hydrolysis to enrich for sphingolipids[26] and the other 2 aliquots were used for glycerophospholipids and phosphorus assay, respectively. Mass spectrometry analysis for the identification and quantification of phospho- and sphingolipid species was performed on a TSQ Vantage Triple Stage Quadrupole Mass Spectrometer (Thermo Fisher Scientific) equipped with a robotic nanoflow ion source (Nanomate HD, Advion Biosciences), using multiple reaction monitoring. Each individual ion dissociation pathway was optimized with regard to collision energy. Lipid concentrations were calculated relative to the relevant internal standards and normalized to the phosphate content of each lipid extract to account for variability in the amount of starting material and to correct for sample loss during the extraction procedure.

Microbiota analysis. DNA extraction. DNA was extracted from about 30 mg colon content using Quick-DNA Fecal/Soil Microbe Miniprep Kit (Zymo). Purified DNA was quantified using the Qubit dsDNA BR Assay Kit (Thermo Fisher Scientific) and stored at −20˚C. Two negative controls were performed by extracting DNA using the same extraction procedure but omitting the addition of colon content.

Amplicon Sequencing. The V3−4 region of the bacterial 16S rRNA genes (*Escherichia coli* positions 341−805) was amplified using 1 ng of DNA extracted from colon content samples or 5 μL of the DNA extract obtained from negative controls in a 25 μL volume of ZymoBIOMICS PCR PreMix (Zymo Research) containing each of 0.4 μM forward primer 5'-barcode-CCTACGGGNGGCWGCAG-3' and reverse primer 5'-barcode-GACTACHVGGGTATCTAATCC-3' tagged with 8-nt barcodes at their 5'ends (Fasteris, Plan-les-Ouates, Switzerland). The PCRs were carried out with an initial denaturation at 95˚C for 3 minutes, followed by 30 cycles of denaturation at 95˚C for 30 seconds, annealing at 51˚C for 30 seconds, and extension at 72˚C for 60 seconds, and a final extension at 72˚C for 10 minutes. Duplicate PCRs of each sample were combined and run (1 μL) on a 2100 Bioanalyzer (Agilent Technologies) for quality analysis and quantification. The sequencing library was constructed using the MetaFast protocol (Fasteris, Plan-les-Ouates, Switzerland). The sequencing was carried out for 2 × 300 cycles on an Illumina MiSeq instrument using MiSeq Reagent Kit v3.

Bioinformatics analysis. Libraries were demultiplexed using the Fasteris internal software. No mismatches were allowed in a barcode and a maximum of 2 mismatches were allowed per 16S primer sequences. Trimmomatic v.0.32[27] was used to remove Illumina adapters and to trim reads, by cutting them once the average quality within the 4-base window fell below a quality score of 15. Reads with a final length <60 bases were discarded. Forward and reverse reads were further quality-filtered and paired-end-joined with PEAR v.0.9.11[28] using the following settings: maximum assembly length (−m) 470; minimum assembly length (−n) 390; minimum overlap (−v) 20; minimum read size after trimming (−t) 240; P value (−P) 0.0001; maximal proportion of uncalled bases (−u) 0; and quality score threshold in trimming (−q) 33. The merged sequences were subjected to the UPARSE pipeline (USEARCH v.8.1.1861)[29] for clustering into operational taxonomic units (OTUs) at 97% identity. Taxonomic assignment of the representative OTUs was performed using MOTHUR v.1.39.5[30] classify.seqs command (with method = wang, −cutoff = 80) and the EzBioCloud 16S rRNA gene sequence database[31] downloaded on 4 January 2018. We removed OTUs that (1) had an average relative abundance higher in the negative controls than in colon content samples or (2) had <90% identity to reference prokaryotic EzBioCloud 16S sequences as revealed by USEARCH (-usearch_global -id 0.9 -query_cov 0.99).[32] Normalization of OTU counts for sequencing depth (110,000) was performed using the "rrarefy" command from the R vegan package. Sequencing data were submitted to the European Nucleotide Archive (ENA; www.ebi.ac.uk/ena; study number: PRJEB36797).

Statistical analyses. Statistical analyses of the data using 1-way ANOVA was performed using the GraphPad Prism version 7.02 software. Graphs represent mean + standard error of the mean (SEM). Clustered heat map was generated in R using the heatmap.2 function of the "gplots" package. A P value < 0.05 was considered statistically significant.

RESULTS

Liraglutide does not change energy homeostasis or carbohydrate metabolism in mice on an MCD diet. First, we investigated the metabolic action of liraglutide in the nutritional context of the MCD-diet. Previous studies have shown that GLP-1Ra, like liraglutide, reduce food intake in rodents.[33] Here, we confirmed that mice fed an MCD-diet eat approximately 30% less than mice fed a chow diet (Fig 2A). Nevertheless, liraglutide did not potentiate the anorexic effect of the MCD-diet.

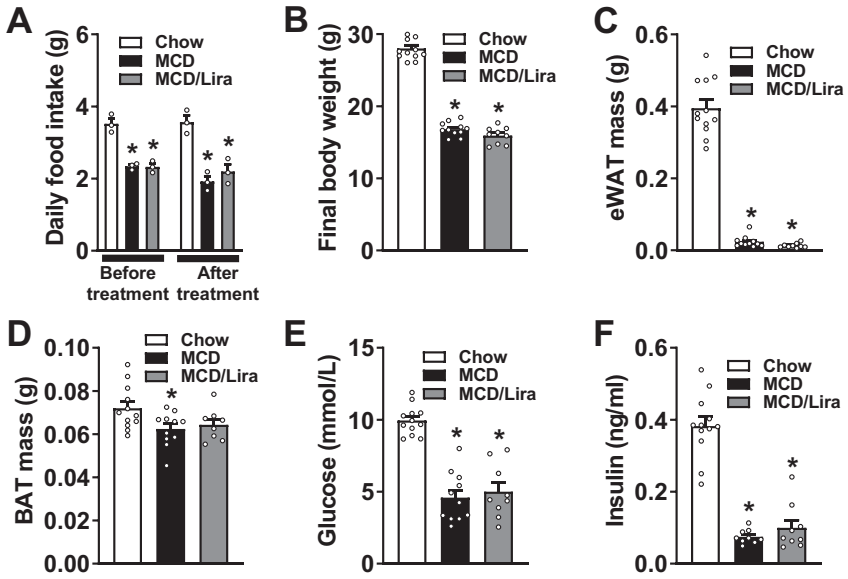

Fig 2. Liraglutide infusion does not modify energy homeostasis or carbohydrate metabolism in mice fed a MCD diet. (A) Food intake before and after saline/liraglutide infusion (g per day). (B) Body weight at the end of the experiment (after 7 weeks of chow/MCD-diet consumption and 4 weeks of saline/liraglutide infusion) (g). (C) Epididymal white adipose tissue (eWAT) mass (g). (D) Brown adipose tissue (BAT) mass (g). (E) Circulating glucose levels (mmol/L). (F) Circulating insulin levels (ng/mL). Results are expressed as the mean ± SEM. n = 9−12 male mice per group. One-way ANOVA: **P* value for MCD or MCD/Lira vs Chow < 0.05, $^{\#}P$ value for MCD/Lira vs MCD < 0.05.

In fact, MCD diet-fed mice infused with liraglutide ate the same amount of food as those infused with saline solution (Fig 2A). Similarly, body weight (Fig 2B), epididymal white adipose tissue mass (Fig 2C), interscapular brown adipose tissue mass (Fig 2D), glycemia (Fig 2E), and insulinemia (Fig 2F) were all significantly decreased by the MCD-diet consumption but unaffected by liraglutide administration. The homeostasis model assessment index, considered as a good marker of whole body insulin sensitivity, was greatly improved in the MCD-diet group but unchanged by liraglutide (Chow: 28.9 ± 1.8, MCD: 2.5 ± 0.5, MCD/Lira: 4.3 ± 1.4, *P*= 0.22 for MCD/Lira vs MCD groups). Taken together, these results showed that liraglutide infusion did not impact energy homeostasis or basal glycemic control in mice on the MCD-diet, allowing us to investigate directly the hepatic action of liraglutide independently of potentially confounding metabolic effects.

Liraglutide changes hepatic lipid composition qualitatively but not quantitatively. Relative liver weight was not statistically different between Chow, MCD and MCD/Lira groups (Fig 3A). Circulating levels of alanine aminotransferase (Fig 3B), aspartate aminotransferase (Fig 3C) and free fatty acids (Fig 3D), increased significantly by the MCD-diet, were not further modified by liraglutide treatment. Similarly, hypocholesterolemia (Fig 3E) and hypotriglyceridemia (Fig 3F) were comparable in MCD diet-fed mice infused with saline solution or liraglutide. As expected, histological hepatic sections stained with H&E and Oil-red O revealed that livers of MCD diet-fed mice displayed significant steatosis and lobular inflammation, while their hepatocytes presented only mild ballooning (Fig 3G, J). Lipids, representing more than 20% of the liver area in MCD diet-fed mice (Fig 3G, H), mostly accumulated as single droplets (ie, macrosteatosis; Fig 3G, I). Liraglutide infusion did not quantitatively affect hepatosteatosis in MCD diet-fed mice (Fig 3G−J), in accordance with unchanged gene expression of central regulators of lipid metabolism (Fig 3K). Nevertheless, lipid species differ in terms of lipotoxicity.[34,35] To evaluate potential changes in lipid composition, we analyzed the hepatic content of over 900 lipid species by targeted mass spectrometry. Hierarchical clustering analysis based on fold-change compared to the Chow group (Fig 4A) highlighted lipid species significantly changed between the MCD and the MCD/Lira groups. Interestingly, the marked increases in C16 and C24-ceramide (Fig 4B) and sphingomyelins (Fig 4C) levels observed in the liver of MCD diet-fed mice were partly alleviated in the liver of MCD diet-fed mice treated with liraglutide. Different biochemical pathways (*de novo* ceramide biosynthesis vs degradation of sphingomyelin into ceramide) converge toward the generation of ceramide (Fig 4D).

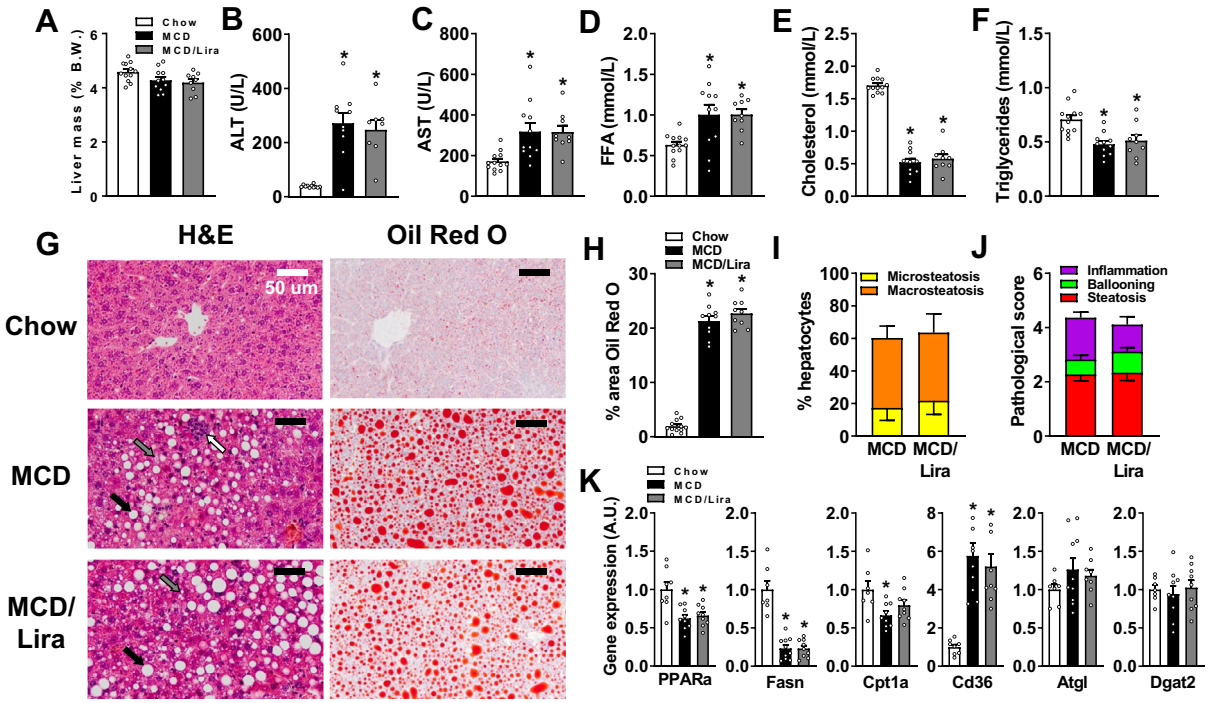

Fig 3. Liraglutide infusion does not quantitatively change hepatic lipid accumulation in MCD diet-fed mice. (A) Relative liver mass (expressed as percentage of body weight). (B) Circulating alanine aminotransferase (ALT) levels (U/L). (C) Circulating aspartate aminotransferase (AST) levels (U/L). (D) Circulating free fatty acid (FFA) levels (mmol/L). (E) Circulating total cholesterol levels (mmol/L). (F) Circulating triglyceride levels (mmol/L). (G) Haematoxylin and eosin (H&E) and Oil-red O staining of liver sections. Scale bars 50 μm, black arrows: macrosteatosis, grey arrow: microsteatosis, white arrows: immune cell infiltration. (H) Quantification of lipids expressed as percent of area of liver sections stained with Oil red O. (I) Evaluation of the percent of hepatocyte containing micro- and macrosteatosis. (J) Pathological score with steatosis and activity (lobular inflammation + ballooning) evaluated by a pathologist blinded to the diets and treatments. (K) Hepatic gene expression of lipids enzymes and transporters (A.U). Results are expressed as the mean ± SEM. n = 9−10 male mice per group (panel A-J), n = 7−9 male mice per group (panel K). One-way ANOVA: **P* value for MCD or MCD/Lira vs Chow < 0.05, $^{\#}P$ value for MCD/Lira vs MCD < 0.05.

Gene expression of key enzymes involved in ceramide production was increased in MCD diet-fed mice compared to mice fed with a chow diet (Fig 4E). Furthermore, gene expression of Sptlc2, cerS4, and cerS6 was downregulated by liraglutide, suggesting a broad effect on sphingolipid metabolism.

Beyond their structural function, the degree of fatty acid saturation of lipid species also impacts the hepatic status.[36-38] To analyze the degree of fatty acid saturation/desaturation, we measured the levels of phospholipids harboring (1) only 1 double bond in both fatty acyl chains combined (considered as monounsaturated fatty acids, MUFA); (2) between 2−6 double bonds in their 2 fatty acyl chains (considered as polyunsaturated fatty acids, PUFA); and (3) no double bonds in their 2 fatty acyl chains (considered as saturated fatty acids, SFA). Hepatic PUFA lipids showed a trend to decrease in MCD/Lira mice compared to chow diet-fed mice while MUFA lipids were similarly decreased in the MCD and MCD/Lira groups compared to the Chow group (Fig 4F). Saturated fatty acid containing lipids were specifically decreased in the MCD/Lira group compared to the Chow and MCD groups (Fig 4F). Among qualitative changes in lipid composition, the length of the fatty acid chain is another important feature for cell membrane permeability/fluidity.[35] Phospholipids with long chains (LC), harboring a combined carbon number of 28−34 in both fatty acyl chains, were reduced in both the MCD and MCD/Lira groups (Fig 4G). In contrast, phospholipids with very long chains (VLC), harboring 38−44 carbons, remained unchanged in the Chow, MCD, and MCD/Lira groups (Fig 4G).

Liraglutide limits inflammation and initiation of fibrosis in mice on an MCD-diet. To further explore the pathology of hepatic inflammatory infiltrates in the MCD/Lira and the MCD groups of mice, we extended the analysis to expression of immune cell markers by means of quantitative real-time PCR. In the liver, macrophages are considered key players, even initiators, of the inflammatory process and are classified according to

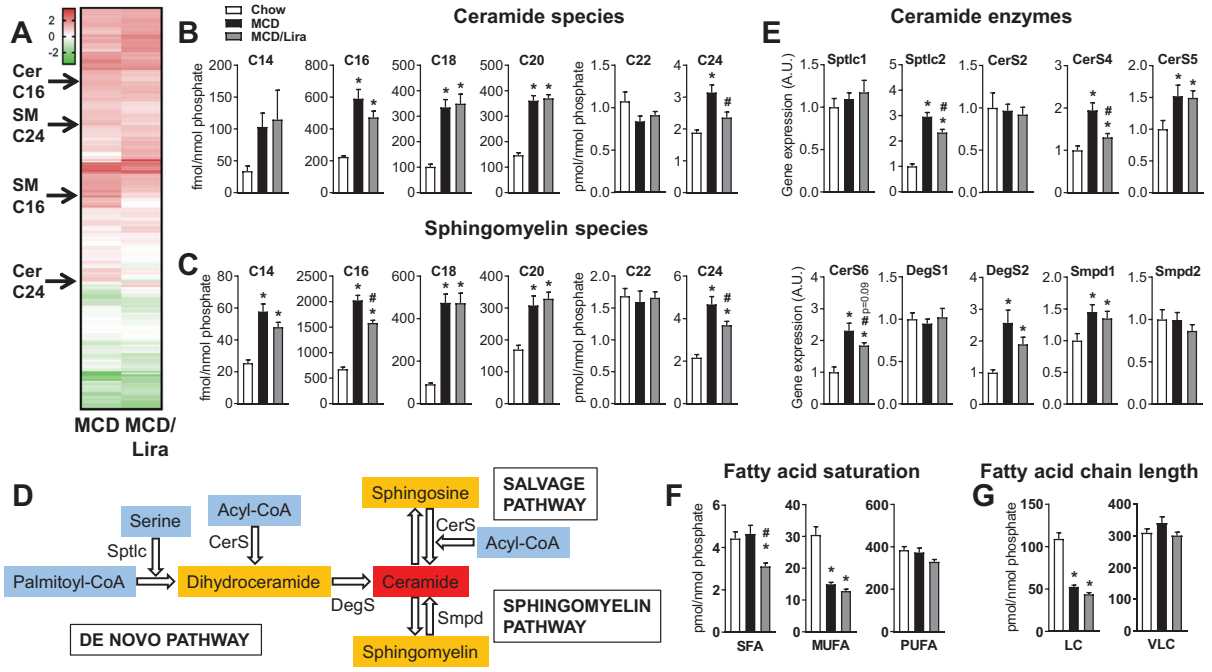

Fig 4. Liraglutide infusion qualitatively changes hepatic lipid composition in MCD diet-fed mice. (A) Hierarchical clustering of 797 lipid hepatic species presented as LOG2 of fold-change compared to the Chow diet group. Most relevant lipid species changed by liraglutide infusion are listed on the left. (B) Concentration of hepatic ceramides normalized to the phosphate content. (C) Concentration of hepatic sphingomyelins normalized to the phosphate content. (D) Schematic representation of biochemical pathways leading to ceramide production. (E) Hepatic gene expression of enzymes involved in the ceramide biosynthesis. (F) Total amount of hepatic phospholipids according to their degree of saturation (normalized to the phosphate content). (G) Total amount of hepatic phospholipids according to their chain length (normalized to the phosphate content). Results are expressed as the mean ± SEM. n = 5−6 male mice per group. Cer, ceramide, SM, sphingomyelin, SFA, saturated fatty acids, MUFA, monounsaturated fatty acids, PUFA, polyunsaturated fatty acids. Diacyl phospholipids were sorted into those that have no double bonds in their 2 fatty acyl chains combined (SFA), one double bond (MUFA) or 2−6 double bonds. LC: long chains (total sum of 28−34 carbons in both fatty acyl chains), VLC: very long chains (total sum of 36−44 carbons in both fatty acyl chains). One-way ANOVA: **P* value for MCD or MCD/Lira vs Chow < 0.05, $^{\#}P$ value for MCD/Lira vs MCD < 0.05.

their tissue of origin or their activation state.[39,40] Molecular markers of both liver-resident Kupffer cells (F4/80, Tlr4, Tlr9) and monocyte-derived macrophages (Ly6c, Ccr2) were all overexpressed in the MCD group and normalized in the MCD/Lira group (Fig 5A). Similarly, markers of classically activated (pro-inflammatory) M1 macrophages (Cd14, Tnfa) were up-regulated in the MCD group and significantly reduced in the MCD/Lira group (Fig 5A). In contrast, no difference was observed between the MCD and the MCD/Lira group regarding the expression of alternatively activated (anti-inflammatory) M2 macrophage markers (Arg1, Cd206, Retnla, Cd163; Fig 5A). Markers of myeloid dendritic cells (Cd11c, MHCII, Cd86; Fig 5, B) and activated hepatic stellate cells (Acta1 and Vim, involved in the deleterious epithelial-mesenchymal transition, Fig 5C) were significantly reduced by liraglutide treatment. In accordance, the expression of several pro-fibrogenic genes was lower in the MCD/Lira group compared to the MCD group (Fig 5D), including Timp1, Serpine1, Mmp13. Even more strikingly, Tgfb1 and genes encoding collagen proteins showed the same basal levels of expression in the MCD/Lira as in the Chow group (Fig 5D). Our experimental set-up (7 weeks of MCD-diet consumption) allowed initiating but not observing a massive fibrosis. Nevertheless, histological staining of hepatic sections with Sirius red showed that the administration of liraglutide reduced the number and the size of collagen fibers in livers of MCD diet-fed mice (Fig 5E). Quantitatively, MCD diet-fed mice exhibited a 7-fold increase in the Sirius red positive area of liver parenchyma compared to mice fed a chow diet (Fig 5F). Per comparison, MCD diet-fed mice treated with liraglutide exhibited a significantly attenuated 4-fold increase in Sirius red positive area compared to chow diet-fed mice (Fig 5F).

Liraglutide impacts the gut-liver axis. As an enterokine, GLP-1 production is regulated by the gut

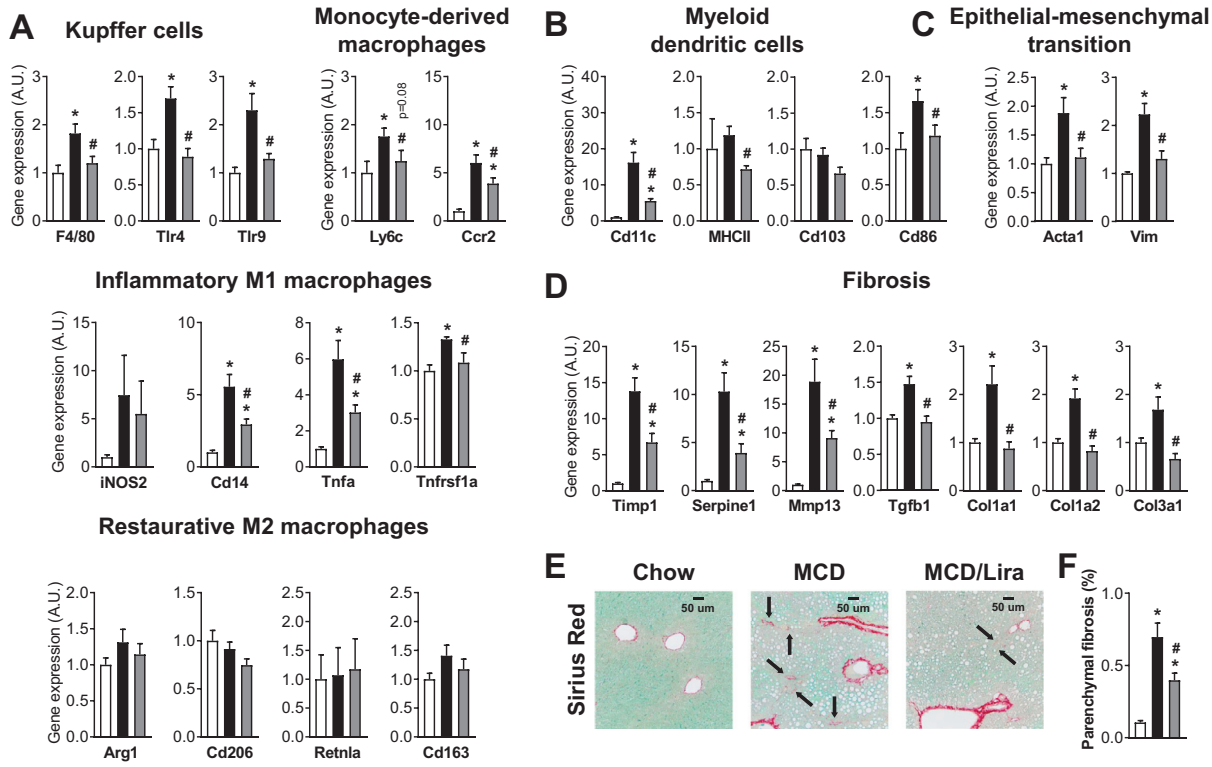

Fig 5. Liraglutide infusion limits hepatic inflammation and initiation of fibrosis in MCD diet-fed mice. Hepatic gene expression of macrophage markers (A), myeloid dendritic cell markers (B), epithelial-mesenchymal transition markers (C), fibrosis markers (D). (E) Sirius red staining of liver sections. Black arrows identify collagen fibers. (F) Quantification of fibrosis expressed as percent of area of parenchymal liver sections stained with Sirius red. Results are expressed as the mean ± SEM. n = 7−10 male mice per group. One-way ANOVA: **P* value for MCD or MCD/Lira vs Chow < 0.05, #*P* value for MCD/Lira vs MCD < 0.05.

microbiota.[41,42] In turn, GLP-1R agonism can modify intestinal bacteria populations.[14,43] In this context, we analyzed and compared the changes in gut microbiota composition in our 3 experimental groups based on sequencing of 16S rRNA gene amplicons. The overall bacterial diversity, measured by the Shannon diversity index, was lower in MCD diet-fed mice, whether treated or not treated with liraglutide (3.37 ± 0.46 and 2.98 ± 0.23, respectively) than in control mice (4.70 ± 0.33). At the phylum level, MCD-diet consumption increased the relative proportion of Firmicutes and massively decreased that of Bacteroidetes (Fig 6A). Among Firmicutes, MCD-diet promoted an overall increase in the relative abundance of the family Erysipelotrichaceae, mostly due to the increase in genera *Turicibacter* and *Allobaculum* while the genus *ASBT* decreased (Fig 6B, C). MCD-diet was also associated with increased relative proportions of Clostridiaceae (notably represented by *Clostridium*), Lactobacillaceae (*Lactobacillus*) and Peptostreptococcaceae (*Romboutsia*) and reduced proportions of Lachnospiraceae (*Eisenbergiella, Clostridium g21*, and *KE159538*; Fig 6C). The global decrease in Bacteroides under MCD-diet was mainly due to a drop in the relative abundance of the family S24-7 and genera belonging to it.

The main effects of liraglutide administration in the MCD nutritional context was the relative increase in *Allobaculum* vs *Turicibacter* and the normalization of the *Bacteroides* content (Fig 6C). Extending the investigations to the gut environment, we observed that gross ileal morphology was markedly impacted by the MCD diet. Villi and crypts were significantly shorter in MCD diet-fed mice compared to chow diet-fed mice (Fig 6D, E). Absolute and relative numbers of proliferative (Ki67-positive) cells were significantly reduced in MCD diet-fed mice whilst liraglutide treatment partially restored the relative proportion of proliferative cells (Fig 6F, G). Finally, the MCD-diet reduced the number of goblet (mucus-producing) cells by 2-fold, which was attenuated by liraglutide infusion (Fig 6H, I).

DISCUSSION

Liraglutide is an efficient antidiabetic drug, recently approved to treat obesity.[44] However, the clinical

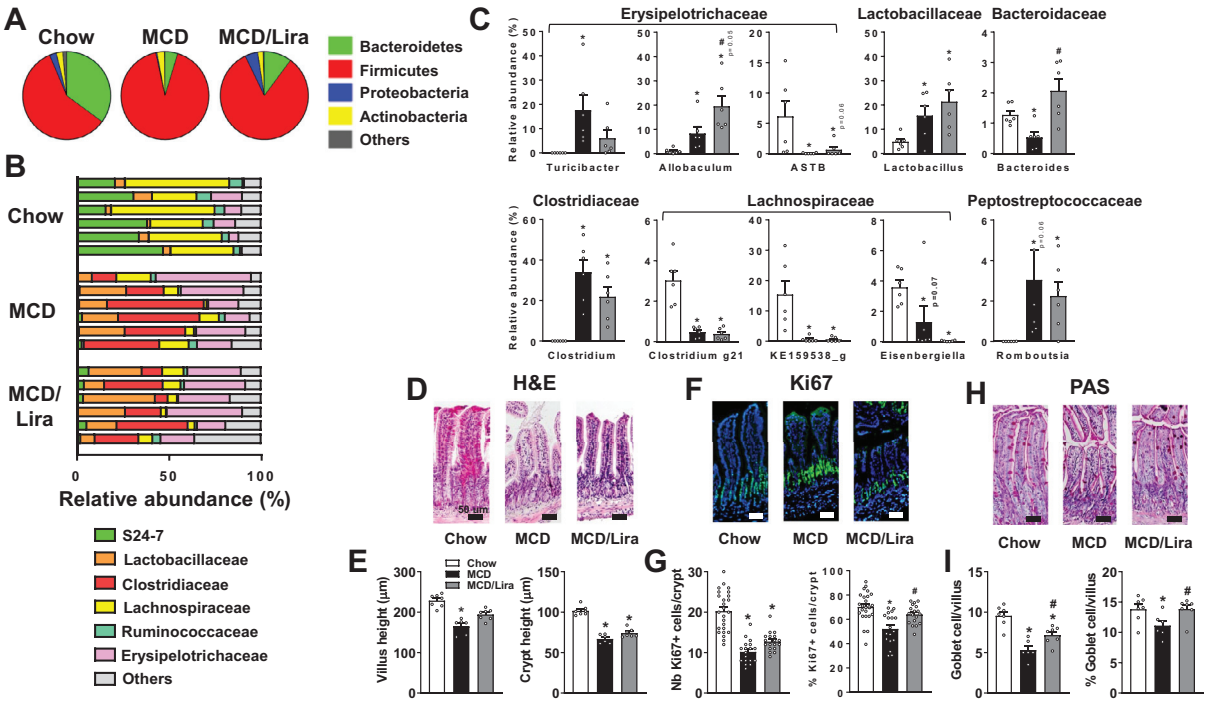

Fig 6. Liraglutide infusion impacts gut microbiota composition and epithelium proliferation in MCD diet-fed mice. Relative abundance of predominant bacterial phyla (A) and families (B) of gut bacteria. (C) Differentially abundant genera between the 3 groups of mice. Histological sections of ileum stained with hematoxylin and eosin (D), Ki67 antibody (F) and Periodic Acid Schiff (H). (E) Quantification of ileal villus and crypt heights (in μm). (G) Quantification of Ki67+ cells per crypt expressed as absolute or relative values. (I) Quantification of goblet cells per villus expressed as absolute or relative values. Results are expressed as the mean ± SEM. n = 6 male mice per group (panel A−C), n = 6−7 male mice per group (panel D-I). One-way ANOVA: **P* value for MCD or MCD/Lira vs Chow < 0.05, $^{\#}P$ value for MCD/Lira vs MCD < 0.05.

impact of liraglutide on NAFLD/NASH remains elusive. Some studies reported an anti-steatotic action in diabetic patients,[22,45-51] but this was not confirmed by other studies.[52,53] In vivo rodent studies also reported anti-steatotic activity of GLP-1Ra, but most often secondary to weight loss or insulin sensitization in situations of positive energy balance, such as in *ob*/*ob* mice,[14] diet-induced obese (DIO) mice[14-16] and DIO-rats.[17-20] In vitro studies suggested that GLP-1Ra exert diverse actions on hepatocytes, including prevention of endoplasmic reticulum stress,[9] activation of AMP-activated protein kinase,[10-12] inhibition of lipogenesis[10] or modulation of insulin signaling.[11-13]

The MCD diet has long been considered a gold standard to study nutritional NASH. This diet also causes an increase in energy expenditure linked to suppression of hepatic expression of stearoyl-coenzyme A desaturase-1 (SCD-1), the enzyme that catalyzes the rate-limiting step in the formation of MUFAs.[54] As MCD diet-fed mice did not respond to peripheral signals (hypolipidemia, hypoglycemia, hypoinsulinemia, hypoleptinemia) aimed at increasing their food intake,[7,54-55] they developed NASH in a state of negative energy balance and weight loss.

Here, we observed that liraglutide does not influence body weight and glycemic parameters in the MCD-diet context, allowing us to dissociate its direct hepatic action from confounding, indirect metabolic effects. First, we observed no change in hepatic neutral lipid storage in response to liraglutide infusion in MCD diet-fed mice. Partitioning of lipid droplets (macro vs micro steatosis) as well as gene expression of lipid enzymes and transporters were also unaffected by liraglutide. Together, these data indicate no direct lipid-lowering action of liraglutide in the liver of this lean NASH model, suggesting that the anti-steatotic action previously observed could be secondary to weight loss and/or improved insulin sensitivity. Nevertheless, beyond the total hepatic lipid content, enrichment in some lipid species/intermediates is linked to liver insulin-resistance and progression of NASH.[56-59] Thus, we extended our investigations to the hepatic lipid composition through LC-MS. This approach revealed that liraglutide could limit the MCD-diet-induced

accumulation of C16 and C24-ceramides/sphingomyelins, confirming previous studies implicating these lipid intermediates in metabolic disorders. In fact, CerS2$^{+/-}$ mice presenting high C16-ceramides levels are prone to diet-induced steatohepatitis and insulin resistance.[60] CerS6 deficiency[61] or silencing,[62] which reduces C16-ceramides levels, allows DIO resistance and improvement in insulin sensitivity and hepatic steatosis. Different pharmacological interventions have also shown a concomitant reduction in ceramide species and amelioration of NASH. Antagonism of peripheral cannabinoid−1 receptor reversed the HFD-induced increase in CerS6 expression and ceramide C16:0 synthase activity.[63] Myriocin, an inhibitor of ceramide synthesis, reduced C16 and C24 ceramides in mice fed a western diet, improving several metabolic parameters including liver fibrosis.[64] To our knowledge, the effect of GLP-1Ra on hepatic ceramide accumulation has not been previously reported. Furthermore, GLP-1Ra Exendin-4 has been shown to prevent ceramide accumulation in cardiac progenitor cells[65] as well as in the heart of Dgat$^{-/-}$ mice.[66] Different biochemical pathways converge towards the generation of ceramide, including de novo ceramide biosynthesis and degradation of sphingomyelin into ceramide.[67] In our study, concomitant upregulation of C16/C24-ceramide and C16/C24-sphingomyelin species, as well as gene expression patterns of Sptlc2 and CerS6, suggest that different sphingolipid pathways are also involved in both the MCD diet-induced ceramide enrichment and, accordingly, ceramide suppression induced by liraglutide. This observation is in accordance with studies showing that sphingolipid metabolism leading to ceramide synthesis is upregulated in NAFLD.[68,69]

Ceramides play an important role in NASH via their crosstalk with inflammatory mediators. Chronic inflammation in the liver (in particular the rise in TNF-α levels) can initiate ceramide production in hepatocytes and, in turn, ceramides can increase cytokine secretion.[70] In humans, sphingolipid species also correlate with hepatic inflammation, suggesting a role for these metabolites during progression from steatosis to NASH.[71] Kupffer cells, the liver resident macrophages, are early responders to hepatocyte injuries, driving TNF-α production.[72] This initial inflammatory event seems to be targeted by liraglutide. In fact, the MCD diet-induced overexpression of Kupffer cell markers (F4/80, Tlr4) and Tnfa are, respectively, fully normalized and consistently alleviated by liraglutide infusion. Macrophage polarization is another important process in the control of inflammation. In fact, depending on multiple factors (for example presence of microbes or damaged tissues), macrophages can oscillate between a classically (pro-inflammatory/M1) activated state or an alternatively (anti-inflammatory/M2) activated state.[73] A previous study reported that liraglutide modulates Kupffer cell polarization leading to an anti-inflammatory-M2 status.[74] Nevertheless, even if we presently observe that liraglutide attenuates MCD-diet induced expression of M1 macrophage markers, we did not detect any enrichment in M2 macrophage markers in our liraglutide-treated mice. Taken together, our results show that liraglutide administration promotes hepatic anti-inflammatory action in MCD-diet-fed mice, in line with its anti-inflammatory properties previously described in adiponectin/ApoE deficiency,[75] high-fat/high-cholesterol diets[18,76] and diabetic patients.[21,46,77-79]

A prolonged pro-inflammatory status can trigger fibrosis, a physio-pathological process with an imbalance between extracellular matrix deposition and reabsorption. Importantly, the severity of hepatic fibrosis is an independent predictor of disease evolution and mortality.[80] In addition to anti-inflammatory actions, we observed that liraglutide presents an anti-fibrotic activity. In fact, the expression of the master regulator of fibrosis initiation (Tgfb1) as well as downstream genes mediating epithelial−mesenchymal transition and extracellular matrix remodeling, all increased by the MCD-diet consumption, were alleviated or fully normalized by liraglutide administration. Histologically, our experimental set-up (7 weeks of MCD-diet exposure) allowed us to observe the early stage of collagen accumulation. Collagen fiber deposits in liver parenchyma appear limited by approximately 40% in the liraglutide-treated group. In accordance, a previous study showed suppression of fibrotic phenotypes in MCD diet-fed mice treated with the GLP-1Ra exenatide.[81] In humans, anti-fibrotic properties of liraglutide are still debated. Liraglutide reduced liver fibrosis in obese women with polycystic ovary syndrome[82] and in some cohorts of type 2 diabetic patients[21,77] but not in others.[53] By what means liraglutide could dampen the fibrosis initiation remains an open question. Activation of hepatic stellate cells (HSCs) into proliferative, fibrogenic myofibroblasts is a key step in hepatic fibrosis progress both in experimental models and human liver NASH.[83] Interestingly, liraglutide can directly de-activate HSCs in vitro.[84] Further work is now required to evaluate the role of liraglutide on HSCs biology in vivo, in particular regarding their proliferation, differentiation and survival. In this way, it has been recently shown that GLP-2R is expressed in HSCs and that HSCs activation and fibrosis were increased in livers of Glp2r$^{-/-}$ mice.[85]

Recently, signals from the gut were identified as important contributors to the pathogenesis of liver disorders.[86,87] In particular, the relationship between gut

microbiota and inflammatory status of the liver has been widely studied. Our results showed modulation of hepatic gene expression of Tlr4 and Tlr9 (involved in the coupling between recognition of bacterial compounds and production of pro-inflammatory cytokines), which led us to analyze gut microbiota composition through NGS in our different experimental groups. The most impressive changes in gut microbiota composition, as a result of the MCD-diet consumption, were the reduction in the Bacteroidales S24-7 family, Lachnospiraceae and Erysipelotrichaceae ASTB. In contrast, the MCD-diet led to massive increases in the relative proportions of *Clostridium, Turicibacter, Allobaculum*, and *Lactobacillus* genera. These observations only partially recapitulate changes previously reported in the same nutritional context. A rise in Clostridium and Turicibacter proportions were in agreement with a previous study in MCD diet-fed mice.[88] In contrast, changes in the relative abundance of *Lactobacillus* showed an inverse trend (increase) as compared to earlier studies.[89,90]

Liraglutide treatment allowed for a full recovery of the relative proportion of *Bacteroides* which was decreased by the MCD-diet. Interestingly, several interactions between *Bacteroides* species and the host immune system have been reported,[91-93] suggesting that an adequate presence of this bacterial genus is required in the microbiota in order to control the inflammatory balance. Among the Erysipelotrichi family, liraglutide treatment also favors the enrichment in *Allobaculum* at the expense of *Turicibacter*. How these microbiome changes contribute to the observed action of liraglutide remains to be elucidated. In fact, technical limitations in the culture of anaerobic bacteria as well as the absence of genera selective antibiotics hinder experimental fine-tuning of gut microbiota composition. Nevertheless, from a translational point of view, it is interesting to note that the relative proportion of *Erysipelotrichi* also correlates with the percentage change in the liver fat content during low choline diet consumption in human clinical studies.[94] Of note, the liraglutide-induced shift in gut microbiota composition appears to be highly diet-dependent. In fact, in response to liraglutide, the main changes observed in HFD-fed mice (concerning *Proteobacteria* and *Akkermansia muciniphila*)[14] are not observed in our MCD diet-fed mice.

By expanding our investigations to the intestine, which represents both a host/microbiota interface and the tissue source of endogenous GLP-1, we observed that liraglutide infusion does not restore villus or crypt height in MCD diet-fed mice. However, liraglutide increased the level of proliferative cells in the crypt, in line with the reversible intestinotrophic action of exendin-4 previously observed in rats[95] and that of liraglutide in mice.[96] This trophic action seems effective under physiological conditions, but not under pathophysiological conditions. In the $Apc^{Min/+}$ mice model of colon cancer, GLP-1Ra did not increase crypt cell proliferation but rather stimulated crypt fission.[97] The preservation of mucus-producing cells, conferred by liraglutide, in the MCD-diet deserves further investigation, in particular to understand if this process could explain the observed change in gut microbiota.

In conclusion, liraglutide treatment led to a concomitant decrease in deleterious ceramide/sphingomyelin species, inflammation and initiation of fibrosis in the liver of MCD diet-fed mice, independently of weight loss and global liver steatosis. These results confirm a direct beneficial hepatic action of the GLP-1Ra liraglutide, with potential translational relevance for T2D patients affected by NASH.

ACKNOWLEDGMENTS

This work was funded by the Gottfried and Julia Bangerter-Rhyner Foundation, unrestricted grant from Novo Nordisk, the Foundation of the Swiss Diabetes Association, the Swisslife Foundation (F.R.J), the Vontobel stiftung, the SNSF grants 189003 (F.R.J), the SNSF grants 310030184708/1 and CRSII3_154405 (C. D.), the Swiss Life Foundation (C.D.), Olga Mayenfisch Foundation (C.D.), and by the Bo & Kerstin Hjelt diabetes Foundation (U.L.-M.). We thank Prof. Jacques Phillippe and his team for practical support and valuable discussions. We also acknowledge Marie-Claude Brulhart Meynet and Florian Visentin for technical assistance, Antoine Poncet for precious advice concerning statistical analysis and Audrey Aebi-Toulotte and Richard James for manuscript language editing. All authors have disclosed potential conflicts of interest and read the journal's policy on conflicts of interest as well as the journal's authorship agreement.

Conflicts of Interest: The authors have declared that no conflict of interest exists.

REFERENCES

1. Rinella ME. Nonalcoholic fatty liver disease: a systematic review. JAMA 2015;313:2263–73.
2. Younossi Z, Anstee QM, Marietti M, et al. Global burden of NAFLD and NASH: trends, predictions, risk factors and prevention. Nat Rev Gastroenterol Hepatol 2018;15:11–20.
3. Michelotti GA, Machado MV, Diehl AM. NAFLD, NASH and liver cancer. Nat Rev Gastroenterol Hepatol 2013;10:656–65.
4. Hebbard L, George J. Animal models of nonalcoholic fatty liver disease. Nat Rev Gastroenterol Hepatol 2011;8:35–44.
5. Yao ZM, Vance DE. Reduction in VLDL, but not HDL, in plasma of rats deficient in choline. Biochem Cell Biol 1990;68:552–8.

6. Weltman MD, Farrell GC, Liddle C. Increased hepatocyte CYP2E1 expression in a rat nutritional model of hepatic steatosis with inflammation. Gastroenterology 1996;111:1645–53.
7. Rinella ME, Green RM. The methionine-choline deficient dietary model of steatohepatitis does not exhibit insulin resistance. J Hepatol 2004;40:47–51.
8. Drucker DJ. Mechanisms of action and therapeutic application of glucagon-like peptide-1. Cell Metab 2018;27:740–56.
9. Sharma S, Mells JE, Fu PP, Saxena NK, Anania FA. GLP-1 analogs reduce hepatocyte steatosis and improve survival by enhancing the unfolded protein response and promoting macroautophagy. PLoS One 2011;6:e25269.
10. Ben-Shlomo S, Zvibel I, Shnell M, et al. Glucagon-like peptide-1 reduces hepatic lipogenesis via activation of AMP-activated protein kinase. J Hepatol 2011;54:1214–23.
11. Svegliati-Baroni G, Saccomanno S, Rychlicki C, et al. Glucagon-like peptide-1 receptor activation stimulates hepatic lipid oxidation and restores hepatic signalling alteration induced by a high-fat diet in nonalcoholic steatohepatitis. Liver Int 2011;31:1285–97.
12. Wang YG, Yang TL. Liraglutide reduces fatty degeneration in hepatic cells via the AMPK/SREBP1 pathway. Exp Ther Med 2015;10:1777–83.
13. Gupta NA, Mells J, Dunham RM, et al. Glucagon-like peptide-1 receptor is present on human hepatocytes and has a direct role in decreasing hepatic steatosis in vitro by modulating elements of the insulin signaling pathway. Hepatology 2010;51:1584–92.
14. Moreira GV, Azevedo FF, Ribeiro LM, et al. Liraglutide modulates gut microbiota and reduces NAFLD in obese mice. J Nutr Biochem 2018;62:143–54.
15. Mells JE, Fu PP, Sharma S, et al. Glp-1 analog, liraglutide, ameliorates hepatic steatosis and cardiac hypertrophy in C57BL/6J mice fed a Western diet. Am J Physiol Gastrointest Liver Physiol 2012;302:G225–35.
16. Zhu W, Feng PP, He K, Li SW, Gong JP. Liraglutide protects non-alcoholic fatty liver disease via inhibiting NLRP3 inflammasome activation in a mouse model induced by high-fat diet. Biochem Biophys Res Commun 2018;505:523–9.
17. Yamazaki S, Satoh H, Watanabe T. Liraglutide enhances insulin sensitivity by activating AMP-activated protein kinase in male Wistar rats. Endocrinology 2014;155:3288–301.
18. Gao H, Zeng Z, Zhang H, et al. The glucagon-like peptide-1 analogue liraglutide inhibits oxidative stress and inflammatory response in the liver of rats with diet-induced non-alcoholic fatty liver disease. Biol Pharm Bull 2015;38:694–702.
19. Decara J, Arrabal S, Beiroa D, et al. Antiobesity efficacy of GLP-1 receptor agonist liraglutide is associated with peripheral tissue-specific modulation of lipid metabolic regulators. Biofactors 2016;42:600–11.
20. Ao N, Yang J, Wang X, Du J. Glucagon-like peptide-1 preserves non-alcoholic fatty liver disease through inhibition of the endoplasmic reticulum stress-associated pathway. Hepatol Res 2016;46:343–53.
21. Armstrong MJ, Gaunt P, Aithal GP, et al. Liraglutide safety and efficacy in patients with non-alcoholic steatohepatitis (LEAN): a multicentre, double-blind, randomised, placebo-controlled phase 2 study. Lancet 2016;387:679–90.
22. Petit JM, Cercueil JP, Loffroy R, et al. Effect of liraglutide therapy on liver fat content in patients with inadequately controlled type 2 diabetes: the lira-NAFLD study. J Clin Endocrinol Metab 2017;102:407–15.
23. Bedossa P, Poitou C, Veyrie N, et al. Histopathological algorithm and scoring system for evaluation of liver lesions in morbidly obese patients. Hepatology 2012;56:1751–9.
24. Loizides-Mangold U, Perrin L, Vandereycken B, et al. Lipidomics reveals diurnal lipid oscillations in human skeletal muscle persisting in cellular myotubes cultured in vitro. Proc Natl Acad Sci U S A 2017;114:E8565–E74.
25. Matyash V, Liebisch G, Kurzchalia TV, Shevchenko A, Schwudke D. Lipid extraction by methyl-tert-butyl ether for high-throughput lipidomics. J Lipid Res 2008;49:1137–46.
26. Clarke NG, Dawson RM. Alkaline O leads to N-transacylation. A new method for the quantitative deacylation of phospholipids. Biochem J 1981;195:301–6.
27. Bolger AM, Lohse M, Usadel B. Trimmomatic: a flexible trimmer for Illumina sequence data. Bioinformatics 2014;30:2114–20.
28. Zhang J, Kobert K, Flouri T, Stamatakis A. PEAR: a fast and accurate Illumina Paired-End reAd mergeR. Bioinformatics 2014;30:614–20.
29. Edgar RCUPARSE. highly accurate OTU sequences from microbial amplicon reads. Nature Methods 2013;10:996–8.
30. Schloss PD, Westcott SL, Ryabin T, et al. Introducing mothur: open-source, platform-independent, community-supported software for describing and comparing microbial communities. Appl Environ Microbiol 2009;75:7537–41.
31. Yoon S-H, Ha S-M, Kwon S, et al. Introducing EzBioCloud: a taxonomically united database of 16S rRNA gene sequences and whole-genome assemblies. Int J Syst Evol Microbiol 2017;67:1613–7.
32. Edgar RC. Search and clustering orders of magnitude faster than BLAST. Bioinformatics 2010;26:2460–1.
33. Kanoski SE, Hayes MR, Skibicka KP. GLP-1 and weight loss: unraveling the diverse neural circuitry. Am J Physiol Regul Integr Comp Physiol 2016;310:R885–95.
34. Liangpunsakul S, Chalasani N. Lipid mediators of liver injury in nonalcoholic fatty liver disease. Am J Physiol Gastrointest Liver Physiol 2019;316:G75–81.
35. Musso G, Cassader M, Paschetta E, Gambino R. Bioactive lipid species and metabolic pathways in progression and resolution of nonalcoholic steatohepatitis. Gastroenterology 2018;155:282–302, e8.
36. Mantzaris MD, Tsianos EV, Galaris D. Interruption of triacylglycerol synthesis in the endoplasmic reticulum is the initiating event for saturated fatty acid-induced lipotoxicity in liver cells. FEBS J 2011;278:519–30.
37. Nivala AM, Reese L, Frye M, Gentile CL, Pagliassotti MJ. Fatty acid-mediated endoplasmic reticulum stress in vivo: differential response to the infusion of Soybean and Lard Oil in rats. Metabolism 2013;62:753–60.
38. Gentile CL, Pagliassotti MJ. The role of fatty acids in the development and progression of nonalcoholic fatty liver disease. J Nutr Biochem 2008;19:567–76.
39. Li C, Xu MM, Wang K, Adler AJ, Vella AT, Zhou B. Macrophage polarization and meta-inflammation. Transl Res 2018;191:29–44.
40. Kazankov K, Jorgensen SMD, Thomsen KL, et al. The role of macrophages in nonalcoholic fatty liver disease and nonalcoholic steatohepatitis. Nat Rev Gastroenterol Hepatol 2019;16:145–59.
41. Hwang I, Park YJ, Kim YR, et al. Alteration of gut microbiota by vancomycin and bacitracin improves insulin resistance via glucagon-like peptide 1 in diet-induced obesity. FASEB J 2015;29:2397–411.
42. Wichmann A, Allahyar A, Greiner TU, et al. Microbial modulation of energy availability in the colon regulates intestinal transit. Cell Host Microbe 2013;14:582–90.
43. Montandon SA, Jornayvaz FR. Effects of antidiabetic drugs on gut microbiota composition. Genes (Basel) 2017;8:250.

44. Knudsen LB, Lau J. The discovery and development of liraglutide and semaglutide. Front Endocrinol (Lausanne) 2019;10:155.
45. Cuthbertson DJ, Irwin A, Gardner CJ, et al. Improved glycaemia correlates with liver fat reduction in obese, type 2 diabetes, patients given glucagon-like peptide-1 (GLP-1) receptor agonists. PLoS One 2012;7:e50117.
46. Bouchi R, Nakano Y, Fukuda T, et al. Reduction of visceral fat by liraglutide is associated with ameliorations of hepatic steatosis, albuminuria, and micro-inflammation in type 2 diabetic patients with insulin treatment: a randomized control trial. Endocr J 2017;64:269–81.
47. Armstrong MJ, Hull D, Guo K, et al. Glucagon-like peptide 1 decreases lipotoxicity in non-alcoholic steatohepatitis. J Hepatol 2016;64:399–408.
48. Feng W, Gao C, Bi Y, et al. Randomized trial comparing the effects of gliclazide, liraglutide, and metformin on diabetes with non-alcoholic fatty liver disease. J Diabetes 2017;9:800–9.
49. Tian F, Zheng Z, Zhang D, He S, Shen J. Efficacy of liraglutide in treating type 2 diabetes mellitus complicated with non-alcoholic fatty liver disease. Biosci Rep 2018:38.
50. Yan J, Yao B, Kuang H, et al. Liraglutide, sitagliptin, and insulin glargine added to metformin: the effect on body weight and intrahepatic lipid in patients with type 2 diabetes mellitus and nonalcoholic fatty liver disease. Hepatology 2019;69:2414–26.
51. Khoo J, Hsiang J, Taneja R, Law NM, Ang TL. Comparative effects of liraglutide 3 mg vs structured lifestyle modification on body weight, liver fat and liver function in obese patients with non-alcoholic fatty liver disease: a pilot randomized trial. Diabetes Obes Metab 2017;19:1814–7.
52. Tang A, Rabasa-Lhoret R, Castel H, Wartelle-Bladou C, et al. Effects of insulin glargine and liraglutide therapy on liver fat as measured by magnetic resonance in patients with type 2 diabetes: a randomized trial. Diabetes Care 2015;38:1339–46.
53. Smits MM, Tonneijck L, Muskiet MH, et al. Twelve week liraglutide or sitagliptin does not affect hepatic fat in type 2 diabetes: a randomised placebo-controlled trial. Diabetologia 2016;59:2588–93.
54. Rizki G, Arnaboldi L, Gabrielli B, et al. Mice fed a lipogenic methionine-choline-deficient diet develop hypermetabolism coincident with hepatic suppression of SCD-1. J Lipid Res 2006;47:2280–90.
55. Leclercq IA, Lebrun VA, Starkel P, Horsmans YJ. Intrahepatic insulin resistance in a murine model of steatohepatitis: effect of PPARgamma agonist pioglitazone. Lab Invest 2007;87:56–65.
56. Camporez JP, Asrih M, Zhang D, et al. Hepatic insulin resistance and increased hepatic glucose production in mice lacking Fgf21. J Endocrinol 2015;226:207–17.
57. Jornayvaz FR, Shulman GI. Diacylglycerol activation of protein kinase Cepsilon and hepatic insulin resistance. Cell Metab 2012;15:574–84.
58. Kawano Y, Nishiumi S, Saito M, Yano Y, Azuma T, Yoshida M. Identification of lipid species linked to the progression of non-alcoholic fatty liver disease. Curr Drug Targets 2015;16:1293–300.
59. Zhang C, Klett EL, Coleman RA. Lipid signals and insulin resistance. Clin Lipidol 2013;8:659–67.
60. Raichur S, Wang ST, Chan PW, et al. CerS2 haploinsufficiency inhibits beta-oxidation and confers susceptibility to diet-induced steatohepatitis and insulin resistance. Cell Metab 2014;20:687–95.
61. Turpin SM, Nicholls HT, Willmes DM, et al. Obesity-induced CerS6-dependent C16:0 ceramide production promotes weight gain and glucose intolerance. Cell Metab 2014;20:678–86.
62. Raichur S, Brunner B, Bielohuby M, et al. The role of C16:0 ceramide in the development of obesity and type 2 diabetes: CerS6 inhibition as a novel therapeutic approach. Mol Metab 2019;21:36–50.
63. Cinar R, Godlewski G, Liu J, et al. Hepatic cannabinoid-1 receptors mediate diet-induced insulin resistance by increasing de novo synthesis of long-chain ceramides. Hepatology 2014;59:143–53.
64. Kasumov T, Li L, Li M, et al. Ceramide as a mediator of non-alcoholic fatty liver disease and associated atherosclerosis. PLoS One 2015;10:e0126910.
65. Leonardini A, D'Oria R, Incalza MA, et al. GLP-1 receptor activation inhibits palmitate-induced apoptosis via ceramide in human cardiac progenitor cells. J Clin Endocrinol Metab 2017;102:4136–47.
66. Liu L, Trent CM, Fang X, et al. Cardiomyocyte-specific loss of diacylglycerol acyltransferase 1 (DGAT1) reproduces the abnormalities in lipids found in severe heart failure. J Biol Chem 2014;289:29881–91.
67. Mullen TD, Hannun YA, Obeid LM. Ceramide synthases at the centre of sphingolipid metabolism and biology. Biochem J 2012;441:789–802.
68. Longato L, Tong M, Wands JR, de la Monte SM. High fat diet induced hepatic steatosis and insulin resistance: role of dysregulated ceramide metabolism. Hepatol Res 2012;42:412–27.
69. Chocian G, Chabowski A, Zendzian-Piotrowska M, Harasim E, Lukaszuk B, Gorski J. High fat diet induces ceramide and sphingomyelin formation in rat's liver nuclei. Mol Cell Biochem 2010;340:125–31.
70. Pagadala M, Kasumov T, McCullough AJ, Zein NN, Kirwan JP. Role of ceramides in nonalcoholic fatty liver disease. Trends Endocrinol Metab 2012;23:365–71.
71. Apostolopoulou M, Gordillo R, Koliaki C, et al. Specific hepatic sphingolipids relate to insulin resistance, oxidative stress, and inflammation in nonalcoholic steatohepatitis. Diabetes Care 2018;41:1235–43.
72. Tosello-Trampont AC, Landes SG, Nguyen V, Novobrantseva TI, Hahn YS. Kuppfer cells trigger nonalcoholic steatohepatitis development in diet-induced mouse model through tumor necrosis factor-alpha production. J Biol Chem 2012;287:40161–72.
73. Murray PJ. Macrophage Polarization. Annu Rev Physiol 2017;79:541–66.
74. Li Z, Feng PP, Zhao ZB, Zhu W, Gong JP, Du HM. Liraglutide protects against inflammatory stress in non-alcoholic fatty liver by modulating Kupffer cells M2 polarization via cAMP-PKA-STAT3 signaling pathway. Biochem Biophys Res Commun 2019;510:20–6.
75. Zhang L, Yang M, Ren H, et al. GLP-1 analogue prevents NAFLD in ApoE KO mice with diet and Acrp30 knockdown by inhibiting c-JNK. Liver Int 2013;33:794–804.
76. Daniels SJ, Leeming DJ, Detlefsen S, et al. Biochemical and histological characterisation of an experimental rodent model of non-alcoholic steatohepatitis - effects of a peroxisome proliferator-activated receptor gamma (PPAR-gamma) agonist and a glucagon-like peptide-1 analogue. Biomed Pharmacother 2019;111:926–33.
77. Ohki T, Isogawa A, Iwamoto M, et al. The effectiveness of liraglutide in nonalcoholic fatty liver disease patients with type 2 diabetes mellitus compared to sitagliptin and pioglitazone. Scient World J 2012;2012:496453.
78. Armstrong MJ, Houlihan DD, Rowe IA, et al. Safety and efficacy of liraglutide in patients with type 2 diabetes and elevated liver enzymes: individual patient data meta-analysis of the LEAD program. Aliment Pharmacol Ther 2013;37:234–42.
79. Eguchi Y, Kitajima Y, Hyogo H, et al. Pilot study of liraglutide effects in non-alcoholic steatohepatitis and non-alcoholic fatty

liver disease with glucose intolerance in Japanese patients (LEAN-J). Hepatol Res 2015;45:269–78.
80. Angulo P, Kleiner DE, Dam-Larsen S, et al. Liver fibrosis, but no other histologic features, is associated with long-term outcomes of patients with nonalcoholic fatty liver disease. Gastroenterology 2015;149:389–97, e10.
81. Zhou M, Mok MT, Sun H, et al. The anti-diabetic drug exenatide, a glucagon-like peptide-1 receptor agonist, counteracts hepatocarcinogenesis through cAMP-PKA-EGFR-STAT3 axis. Oncogene 2017;36:4135–49.
82. Kahal H, Abouda G, Rigby AS, Coady AM, Kilpatrick ES, Atkin SL. Glucagon-like peptide-1 analogue, liraglutide, improves liver fibrosis markers in obese women with polycystic ovary syndrome and nonalcoholic fatty liver disease. Clin Endocrinol (Oxf) 2014;81:523–8.
83. Tsuchida T, Friedman SL. Mechanisms of hepatic stellate cell activation. Nat Rev Gastroenterol Hepatol 2017;14:397–411.
84. de Mesquita FC, Guixe-Muntet S, Fernandez-Iglesias A, et al. Liraglutide improves liver microvascular dysfunction in cirrhosis: Evidence from translational studies. Sci Rep 2017;7:3255.
85. Fuchs S, Yusta B, Baggio LL, Varin EM, Matthews D, Drucker DJ. Loss of Glp2r signaling activates hepatic stellate cells and exacerbates diet-induced steatohepatitis in mice. JCI Insight 2020;5:e136907.
86. Marra F, Svegliati-Baroni G. Lipotoxicity and the gut-liver axis in NASH pathogenesis. J Hepatol 2018;68:280–95.
87. Federico A, Dallio M, Godos J, Loguercio C, Salomone F. Targeting gut-liver axis for the treatment of nonalcoholic steatohepatitis: translational and clinical evidence. Transl Res 2016;167:116–24.
88. Ye JZ, Li YT, Wu WR, et al. Dynamic alterations in the gut microbiota and metabolome during the development of methionine-choline-deficient diet-induced nonalcoholic steatohepatitis. World J Gastroenterol 2018;24:2468–81.
89. Okubo H, Sakoda H, Kushiyama A, et al. Lactobacillus casei strain Shirota protects against nonalcoholic steatohepatitis development in a rodent model. Am J Physiol Gastrointest Liver Physiol 2013;305:G911–8.
90. Okubo H, Nakatsu Y, Sakoda H, et al. Mosapride citrate improves nonalcoholic steatohepatitis with increased fecal lactic acid bacteria and plasma glucagon-like peptide-1 level in a rodent model. Am J Physiol Gastrointest Liver Physiol 2015;308:G151–8.
91. Ivanov II, Frutos Rde L, Manel N, et al. Specific microbiota direct the differentiation of IL-17-producing T-helper cells in the mucosa of the small intestine. Cell Host Microbe 2008;4:337–49.
92. Round JL, Mazmanian SK. Inducible Foxp3+ regulatory T-cell development by a commensal bacterium of the intestinal microbiota. Proc Natl Acad Sci U S A 2010;107:12204–9.
93. Neff CP, Rhodes ME, Arnolds KL, et al. Diverse intestinal bacteria contain putative zwitterionic capsular polysaccharides with anti-inflammatory properties. Cell Host Microbe 2016;20:535–47.
94. Spencer MD, Hamp TJ, Reid RW, Fischer LM, Zeisel SH, Fodor AA. Association between composition of the human gastrointestinal microbiome and development of fatty liver with choline deficiency. Gastroenterology 2011;140:976–86.
95. Simonsen L, Pilgaard S, Orskov C, et al. Exendin-4, but not dipeptidyl peptidase IV inhibition, increases small intestinal mass in GK rats. Am J Physiol Gastrointest Liver Physiol 2007;293:G288–95.
96. Kissow H, Hartmann B, Holst JJ, et al. Glucagon-like peptide-1 (GLP-1) receptor agonism or DPP-4 inhibition does not accelerate neoplasia in carcinogen treated mice. Regul Pept 2012;179:91–100.
97. Koehler JA, Baggio LL, Yusta B, et al. GLP-1R agonists promote normal and neoplastic intestinal growth through mechanisms requiring Fgf7. Cell Metab 2015;21:379–91.